Particle & Particle Systems Characterization
www.particle-journal.com
www.MaterialsViews.com

Growth of Ru-Modified Co_3O_4 Nanosheets on Carbon Textiles toward Flexible and Efficient Cathodes for Flexible Li–O_2 Batteries

*Qing-chao Liu, Ji-jing Xu, Zhi-wen Chang, Dan Xu, Yan-bin Yin, Xiao-yang Yang, Tong Liu, Yin-shan Jiang, Jun-min Yan, and Xin-bo Zhang**

Rechargeable lithium–oxygen (Li–O_2) batteries are emerging as one of the most promising electrochemical energy-storage technologies and have captured the interest of more and more researchers due to thier exceptionally high theoretical energy density, 3600 W h kg^{-1} ($2Li + O_2 = Li_2O_2$, 2.96 V vs Li/Li^+).[1–8] However, research on Li–O_2 is still at the infant stage, and many scientific and technological challenges need to be overcome before it is applied to the next-generation high-energy-storage and portable devices.[9–13] For example, the cathode design should be further optimized to improve the round-trip efficiency and cycling performance, as well as the flexibility of the Li–O_2 battery.[14–19] Currently, the cathode is usually based on carbon materials, including commercial carbon, carbon nanotubes, and graphene, etc.[15,20–22] However, recent reports found that the carbon electrode can react with Li_2O_2 to form Li_2CO_3.[23,24] To avoid this reaction, carbon-free or modified carbon material cathodes are proposed.[25–31] Adding insult to injury, commonly used organic binders (e.g., PVDF) are found to be quite unstable in Li–O_2 batteries.[32–34] Furthermore, the addition of a nonconductive binder inevitably increases the impedance of the cell. Therefore, modification of carbon materials and development of a binder-free cathode are urgently important, but still very challenging. To this end, various noncarbon and/or binder-free cathodes have been developed. However, it should be noted that almost all the cathodes are too rigid and bulky to satisfy the requirements of portable, especially flexible, devices. Thus, it is highly desirable to obtain a stable and flexible cathode that can extend the advantage of the very high theoretical energy density (much higher than that of state-of-the-art lithium-ion batteries, ≈300 W h kg^{-1}) of Li–O_2 batteries for next-generation flexible electronics.[35–39]

Dr. Q.-C. Liu, Dr. J.-J. Xu, Z.-W. Chang,
Dr. D. Xu, Y.-B. Yin, X.-Y. Yang, T. Liu, Prof. X.-B. Zhang
State Key Laboratory of Rare Earth Resource Utilization
Changchun Institute of Applied Chemistry
Chinese Academy of Sciences
Changchun 130022, China
E-mail: xbzhang@ciac.ac.cn
Dr. Q.-C. Liu, Y.-B. Yin, X.-Y. Yang, Prof. Y.-S. Jiang, Prof. J.-M. Yan
School of Materials Science and Engineering
Jilin University
Changchun 130012, China
Z.-W. Chang, T. Liu
University of Chinese Academy of Sciences
Beijing 100049, China

DOI: 10.1002/ppsc.201500193

Here, we have developed a mechanically flexible and highly efficient air cathode based on Ru nanoparticles (Ru NPs) decorated on Co_3O_4 nanosheet (Co_3O_4 NS) arrays vertically grown on flexible carbon textiles (CTs). This cathode was prepared by a simple two-step process involving electro-deposition (step 1) and a subsequent impregnation (step 2) progress, as shown in **Figure 1**. First, Co_3O_4 NSs were directly electrodeposited on CTs, and then the obtained Co_3O_4 NSs were impregnated in $RuCl_3$ solution and calcined in an Ar/H_2 atmosphere. This obtained cathode has many tailored properties: i) the application of Co_3O_4 NSs-Ru as cathode materials has remitted the problems from carbon oxidation; ii) direct growth of Co_3O_4 NSs-Ru on CTs can effectively avoid by-products caused by organic binder decomposition and enhance the electronic conductivity; iii) the introduced Ru NPs as an electrocatalyst can effectively reduce the overpotential and improve the cycling performance;[31,40] iv) the CT substrate endows this cathode with excellent flexible properties, which is one of the main preconditions for the development of flexible Li–O_2 batteries.

Figure 2a shows that the pristine CTs are woven by carbon fibers with a diameter of ≈10 μm. The morphology and structure of the fabricated CTs-Co_3O_4 NSs-Ru are investigated and displayed in Figure 2b,c, it could be found that Co_3O_4 NSs-Ru are grown vertically on the skeletons of the carbon fibers, forming a free-standing and 3D hierarchical structure. The direct growth of active materials on the carbon fiber skeleton is favorable for electron transportation. The open macropores offer sufficient channels to transfer O_2, electrolyte, and reaction intermediate species freely in or out of the inner cathode, which can effectively improve the rate capability of the Li–O_2 battery. Besides, the open macropores can accommodate more discharge products, which can improve the battery capacity. What is more, the open macropores can effectively remit the volume effect caused by the discharge product (Li_2O_2). The N_2-adsorption isotherm and the pore-size distribution are shown in Figure 2d, and a distinct hysteresis loop can be observed with typical IV sorption with a high Brunauer–Emmett–Teller specific surface area of 41 m^2 g^{-1} and the major size of the pores falls into the range of 40–60 nm. Typical TEM images of Co_3O_4 NSs-Ru are exhibited in Figure 2e; it was found that Ru NPs uniformly distribute on the surface of Co_3O_4 NSs with a size of about 2 nm. The Ru content is measured to be 6 wt% by inductively coupled plasma–atomic emission spectrometry (ICP-AES). Due to the small grain size and the low content of Ru, we could not find the peaks of Ru through X-ray diffraction (XRD) (Figure S2, Supporting Information). Figure 2f shows an

© 2016 WILEY-VCH Verlag GmbH & Co. KGaA, Weinheim

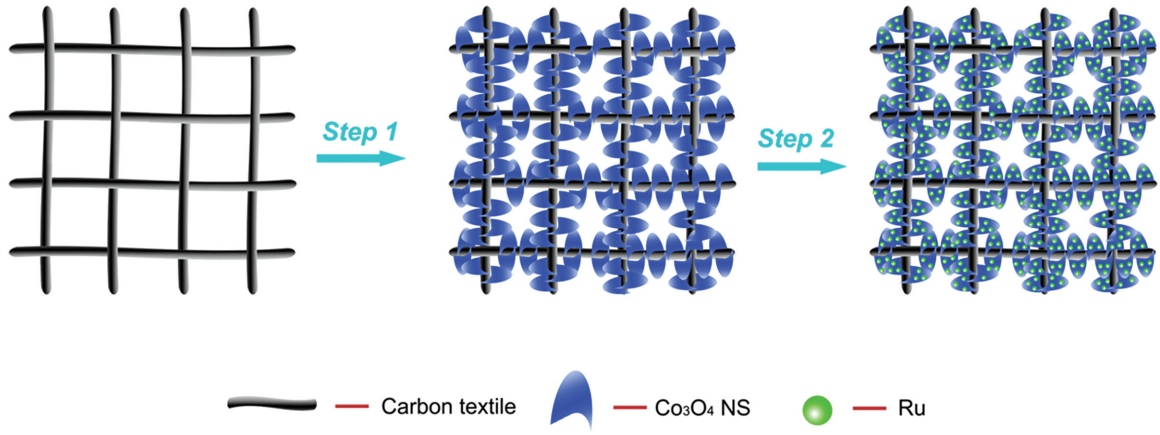

Figure 1. Schematic representations for the design and preparation of the CTs-Co_3O_4 NSs-Ru cathode.

interplanar spacing of ≈0.21 nm, corresponding to the (101) plane of the hexagonal Ru. Energy-dispersive X-ray spectrometry (EDXS) characterization (Figure 2g–i) reveals the existence and homogeneous distribution of the Ru NPs decorated on the surface of Co_3O_4 NSs, which also indicates that the CTs-Co_3O_4 NSs-Ru cathode has been well synthesized.

The electrochemical performance of Li–O_2 cells with CTs-Co_3O_4 NSs and CTs-Co_3O_4 NSs-Ru is displayed in **Figure 3**. In this work, $LiCF_3SO_3$ was dissolved in tetraethylene glycol dimethyl ether (TEGDME) as electrolyte, which is stable against O_2^-.[41–43] To investigate the effect of CTs-Co_3O_4 NSs-Ru on the oxygen reduction reaction (ORR) and oxygen evolution reaction (OER) kinetics, the first discharge–charge curves of the Li–O_2 cells with CTs-Co_3O_4 NSs and CTs-Co_3O_4 NSs-Ru cathodes with the same current density (200 mA g^{-1}) are obtained, which are shown in Figure 3a. The discharge plateau of the cell with the CTs-Co_3O_4 NSs-Ru cathode is higher than that of cell with the CTs-Co_3O_4 NSs cathode by about 10 mV. Surprisingly, the charge overpotential of the cell with CTs-Co_3O_4 NSs-Ru cathode is much lower than the cell with CTs-Co_3O_4 NSs about 550 mV, though the CTs-Co_3O_4 NSs cathode itself possesses electrochemical catalysis compared to pure CTs (Figure S3, Supporting Information). The round-trip efficiency of this battery with the Co_3O_4 NSs-Ru cathode can achieve a value as high as ≈80%. The negligible background discharge capacity of the Li–O_2 cells with pristine CTs, CTs-Co_3O_4 NSs, and CTs-Co_3O_4 NSs-Ru cathodes, which were tested in an argon (Ar) atmosphere, exclude possible electrochemical contributions from intercalation of lithium ions (Li^+) (Figure S4, Supporting Information), demonstrating that the discharge capacities of the Li–O_2 cells are derived from the oxygen reduction. In order to further investigate the catalytic activity of the CTs-Co_3O_4 NSs-Ru, cyclic voltammograms (CVs) of the Li–O_2 cells with CTs-Co_3O_4 NSs and CTs-Co_3O_4 NSs-Ru cathodes were recorded at a scan rate of 0.05 mV s^{-1} (Figure 3b). In the cathodic scan, both samples show typical ORR currents as the potential goes down. In particular, the cell with the CTs-Co_3O_4 NSs-Ru cathode possesses higher onset potential and larger ORR current than that with the CTs-Co_3O_4 NSs cathode, indicating that CTs-Co_3O_4 NSs-Ru has a better ORR catalytic activity. In the anodic scan, the characteristic features of the OER can be observed in both samples. It should be noted that the Li–O_2 cell with the CTs-Co_3O_4 NSs-Ru cathode presents lower onset potentials than the Li–O_2 cell with CTs-Co_3O_4 NSs, which further demonstrates the excellent OER electrocatalytic activity of CTs-Co_3O_4 NSs-Ru when used as a Li–O_2 cathode. Both these results match well with those from Figure 3a. The cycling performance of the Li–O_2 cells with CTs-Co_3O_4 NSs and CTs-Co_3O_4 NSs-Ru were then investigated as shown in Figure 3c–e; the cells were tested by controlling the discharge depth to 1000 mA h g^{-1} at a current density of 200 mA g^{-1}. Figure 3c,d shows the discharge–charge curves of the two cells, and their corresponding cutoff voltages are given in Figure 3e. Surprisingly, it is found that after 72 cycles, the cutoff voltage of the cell with CTs-Co_3O_4 NSs-Ru cathode is still above 2.0 V, while the cell with the CTs-Co_3O_4 NSs cathode could only run for 19 cycles and pure CTs could only sustain 12 cycles (Figure S5, Supporting Information). This excellent cycling performance can be attributed to a series of unique characteristics: the added Ru NPs could effectively improve the catalyst kinetics of the cathode; the unique morphology of the discharge product formed on the cathode provides sufficient electrolyte–Li_2O_2 interfaces that promote the decomposition of Li_2O_2 during charge (vide infra). Besides, the rate performance is also investigated, as displayed in Figure 3f. Interestingly, the discharge capacity at a current density of 1000 mA g^{-1} can still reach as high as 1593 mA h g^{-1}. Furthermore, the Li–O_2 battery with the CTs-Co_3O_4 NSs-Ru cathode also demonstrates excellent performance compared with those in the published literature (Table S1, Supporting Information). To demonstrate its practical applications in flexible energy-storage devices, a flexible Li–O_2 battery was assembled via using this flexible CTs-Co_3O_4 NSs-Ru cathode and used to control a commercial red LED, which could work normally, whether the battery was in planar or bending condition, as displayed in Figure 3g,h.

The morphology variation of the discharged and recharged CTs-Co_3O_4 NSs-Ru cathode and the morphology of the discharge products on the CTs-Co_3O_4 NSs-Ru cathode were then investigated. The capacity was restricted to 1000 mA h g^{-1} and the current density was 200 mA g^{-1}. **Figure 4**a,b show the first discharged morphologies of this cathode, unlike the classical toroidal morphology formed on the pure CTs (Figure S6,

© 2016 WILEY-VCH Verlag GmbH & Co. KGaA, Weinheim

Particle
& Particle Systems Characterization
www.particle-journal.com

Materials Views
www.MaterialsViews.com

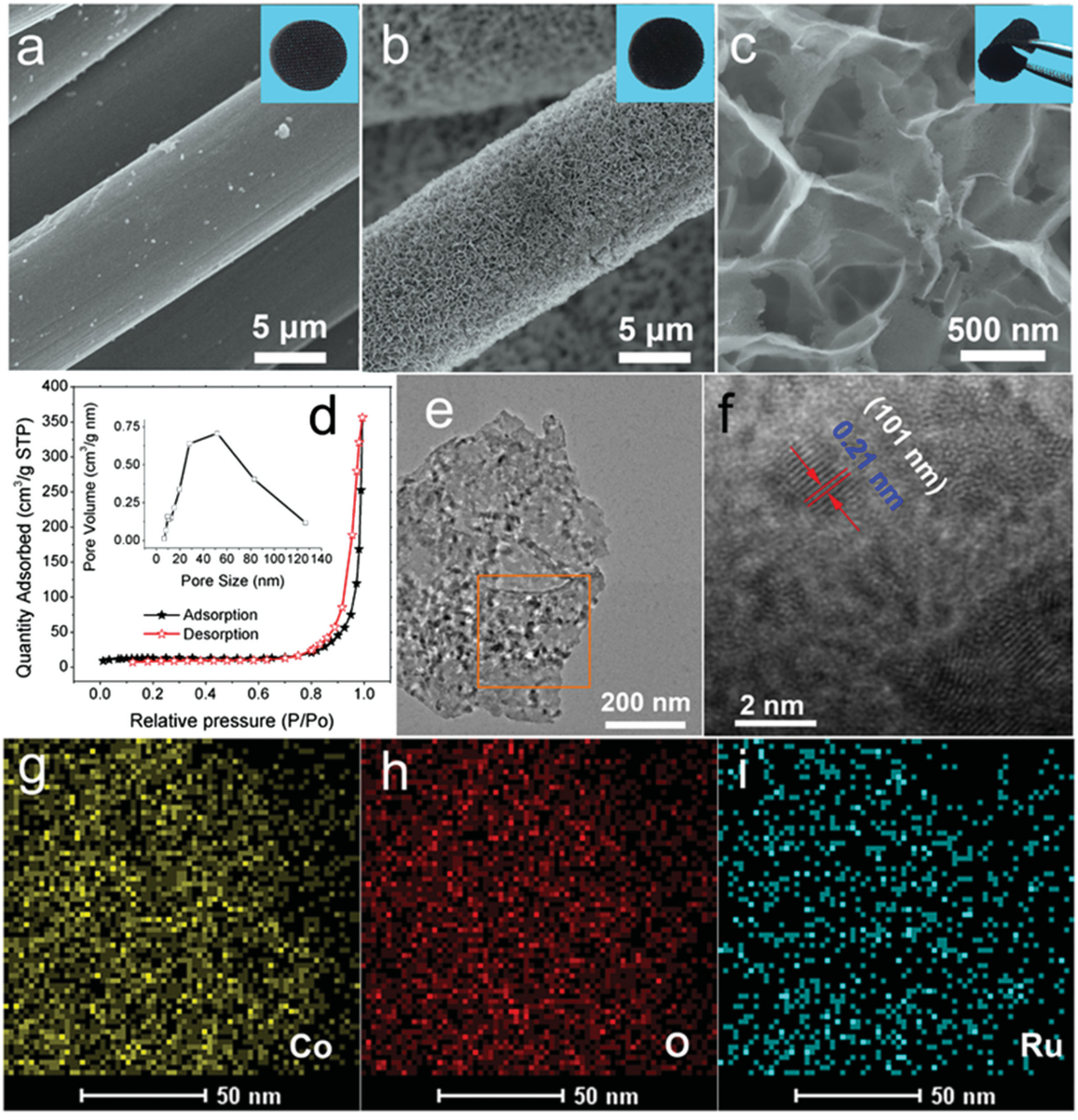

Figure 2. a) SEM image and photograph (inset) of pristine-CTs. b) SEM image and photograph (inset) of the obtained CTs-Co_3O_4 NSs-Ru cathode. c) Higher-magnification image of panel (b); the inset photograph displays the flexible properties of the obtained cathode. d) Nitrogen adsorption–desorption isotherm and pore-size distribution curves (inset). e–h) TEM image (e) and its corresponding EDS mappings (f–h).

Supporting Information),[44–48] the discharge products formed on this cathode are nanosheets that uniformly grow vertically onto the CTs-Co_3O_4 NSs-Ru, which is also different from the disordered discharge products formed on the CTs-Co_3O_4 NSs cathode (Figure S7, Supporting Information). It is considered that Ru or/and Co_3O_4 NSs surfaces are to be less "sticky" than carbon surfaces riddled with dangling bonds, which can weaken the binding of the generated superoxide to the substrate, thus enhancing the diffusion of the superoxide molecules away from the cathode surface favoring the nucleation and crystallization of Li_2O_2 on the preferred crystal faces, and leading to nanosheet-shaped structure growth.[14,45] The uniformly and loosely distributed nanosheets provide sufficient product–electrolyte interfaces, which can promote subsequent charge process and finally enhance the electrochemical performance of the Li–O_2 battery. Simultaneously, the formation of nanosheet Li_2O_2 can also benefit the structural integrity of the CTs-Co_3O_4 NSs-Ru cathode compared with the toroid Li_2O_2 formed on the CTs cathode.[14] After recharging, the discharge product Li_2O_2 disappeared, revealing the rechargeability of the cathode. Fourier transform infrared (FTIR) spectroscopy technology is applied to investigate the discharge products as displayed in Figure 4e: it can be found that the dominant product is Li_2O_2. It should be noted that the discharge product can be almost decomposed during the following recharge process, which is in agreement with the electrochemical impedance spectra (Figure S8, Supporting Information) and SEM results (Figure 4d). For further understanding of the

© 2016 WILEY-VCH Verlag GmbH & Co. KGaA, Weinheim

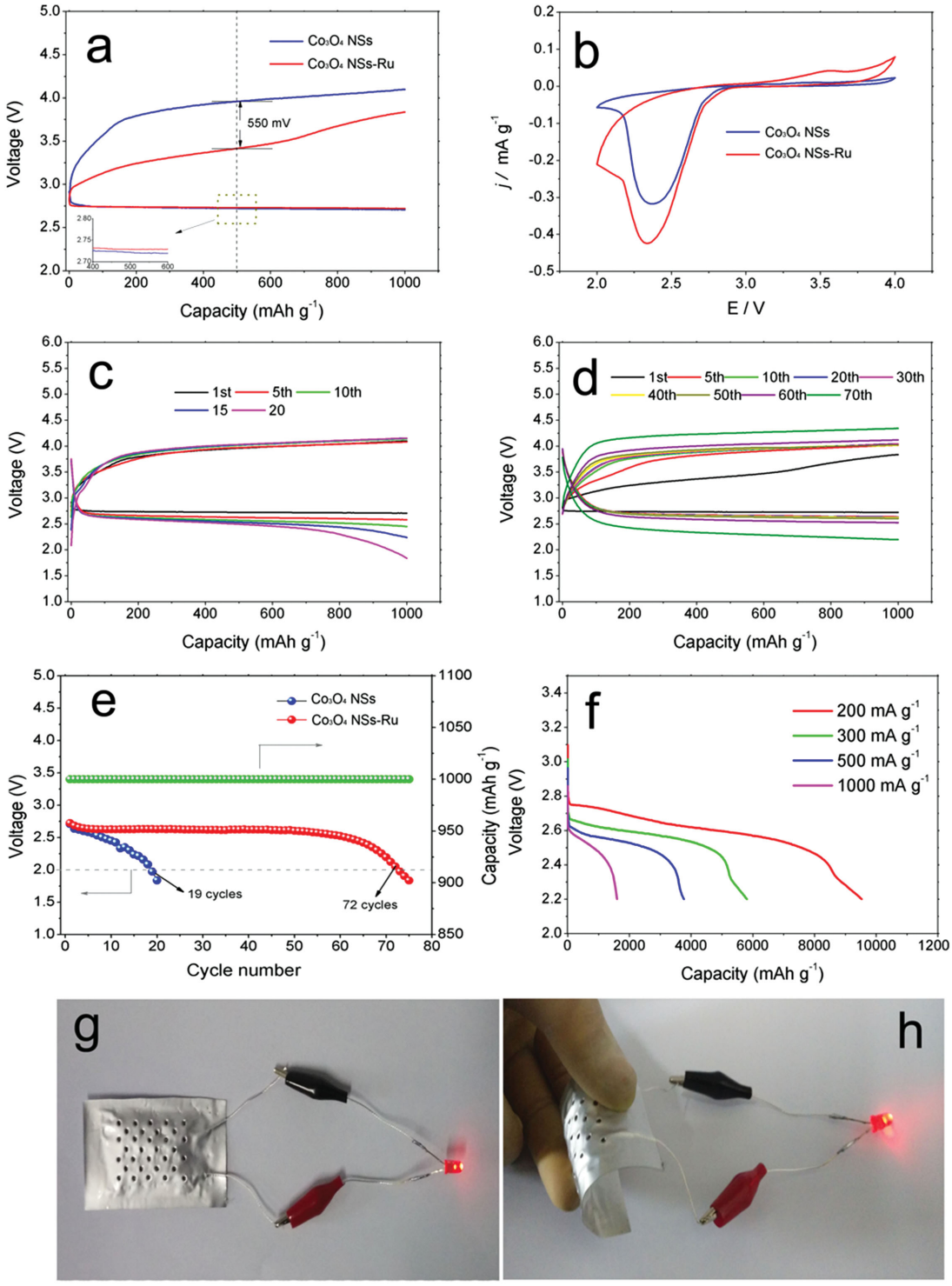

Figure 3. a) First discharge–charge curves of Li–O_2 cells with two different cathodes (CTs-Co_3O_4 NSs and CTs-Co_3O_4 NSs-Ru, respectively) at a fixed capacity of 1000 mA h g^{-1}, b) CVs of Li–O_2 cells with the two kinds of cathodes at a constant scan rate of 0.05 mV s^{-1}. c,d) Cycling performance of the two cells with the capacity limited to 1000 mA h g^{-1}. e) Variation of voltage on the terminal discharge of the Li–O_2 cells with CTs-Co_3O_4 NSs (blue) and CTs-Co_3O_4 NSs-Ru cathode, respectively. f) Rate performance of the cell with two kinds of cathodes. g,h) Digital images of the red LED equipment turned on with the fabricated flexible Li–O_2 battery with planar and bent conditions.

© 2016 WILEY-VCH Verlag GmbH & Co. KGaA, Weinheim

Particle
& Particle Systems Characterization
www.particle-journal.com

Materials Views
www.MaterialsViews.com

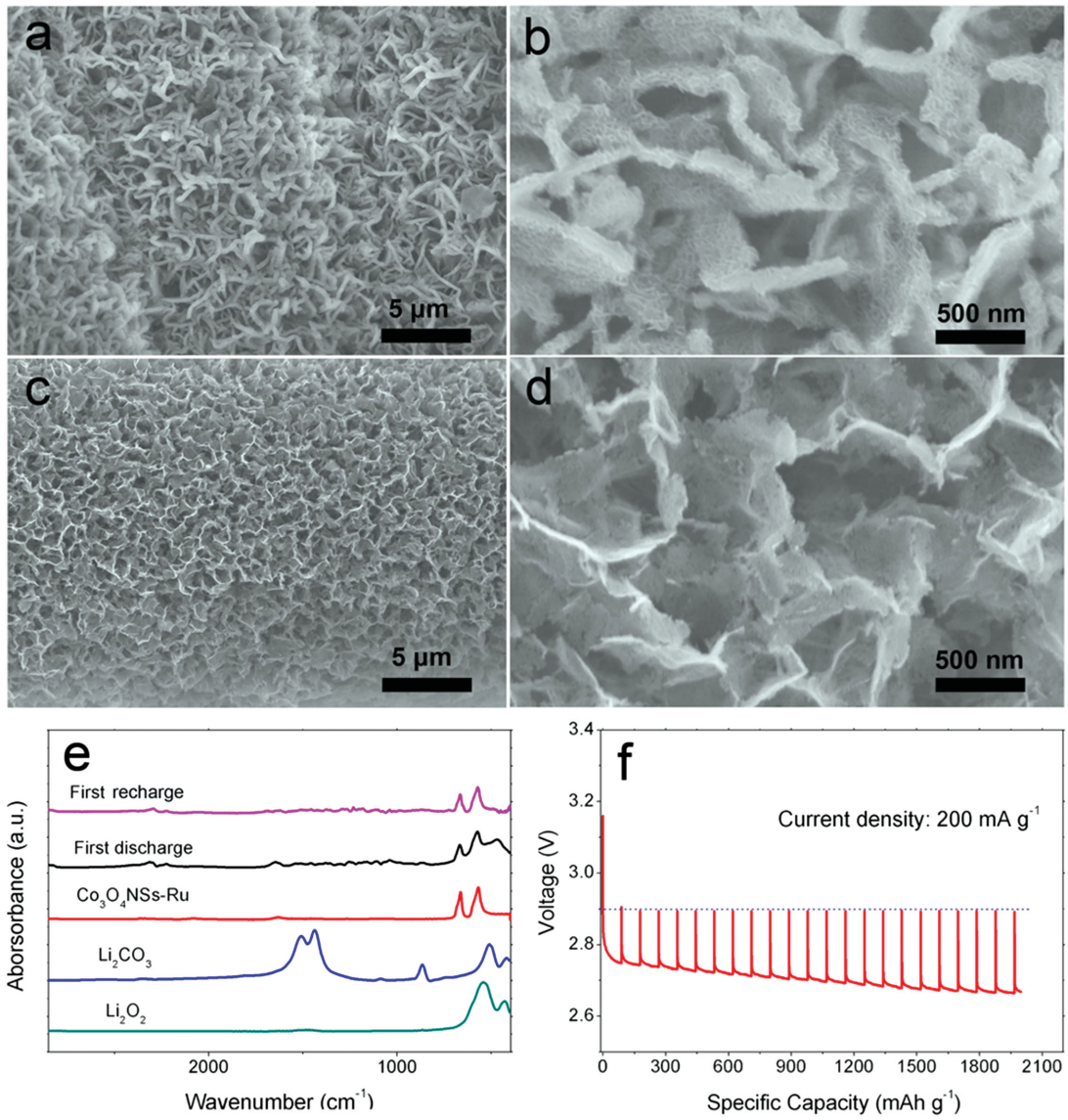

Figure 4. a,c) SEM images of the CTs-Co_3O_4 NSs-Ru cathode on first discharge (a) and after recharge (c). b,d) Higher-magnification images of panels (a) and (c), respectively. e) FTIR spectra of the CTs-Co_3O_4 NSs-Ru cathode on first discharge and after recharge**.** f) GITT discharge voltage profile obtained from the Li–O_2 cell with CTs-Co_3O_4 NSs-Ru cathode.

electrochemical behavior in the Li–O_2 battery, the galvanostatic intermittent titration technique (GITT) is also applied (Figure 4f). The equilibrium potential of the Li–O_2 battery is near 2.9 V, regardless of the state of discharge, and this is the potential for formation of Li_2O_2.[49,50]

In summary, a flexible, noncarbon, dominant free-standing cathode with Ru-decorated Co_3O_4 NSs grown on the CTs was successfully synthesized. With it directly employed as an O_2 cathode, the Li–O_2 battery shows a high capacity, improved round-trip efficiency, and enhanced cycling capability. The excellent electrochemical performance of this battery is ascribed to the reasonable 3D air cathode structure design and the homogeneous distribution of Ru NPs modified on the Co_3O_4 NSs, which tailors the morphology of the discharged product. Besides, due to the flexible properties of this cathode, a novel class of flexible Li–O_2 battery was also assembled, which makes various potential applications possible and opens a door for the use of flexible high-energy-density devices.

Supporting Information

Supporting Information is available from the Wiley Online Library or from the author.

Acknowledgements

This work was financially supported by 100 Talents Program of The Chinese Academy of Sciences, National Program on Key Basic Research Project of China (973 Program, Grant Nos. 2012CB215500 and

© 2016 WILEY-VCH Verlag GmbH & Co. KGaA, Weinheim

2014CB932300), and National Natural Science Foundation of China (Grant Nos. 21101147 and 21203176).

Received: September 25, 2015
Revised: January 4, 2016
Published online: February 4, 2016

[1] K. M. Abraham, Z. Jiang, *J. Electrochem. Soc.* **1996**,*143*, 1.
[2] P. G. Bruce, S. A. Freunberger, L. J. Hardwick, J.-M. Tarascon, *Nat. Mater.* **2012**, *11*, 19.
[3] Y.-C. Lu, H. A. Gasteiger, M. C. Parent, V. Chiloyan, Y. Shao-Horn, *Electrochem. Solid-State Lett.* **2010**, *13*, A69.
[4] J. P. Zheng, R. Y. Liang, M. Hendrickson, E. J. Plichta, *J. Electrochem. Soc* **2008**, *155*, A432.
[5] F. Li, T. Zhang, H. Zhou, *Energy Environ. Sci.* **2013**, *6*, 1125.
[6] Y.-C. Lu, B. M. Gallant, D. G. Kwabi, J. R. Harding, R. R. Mitchell, M. S. Whittingham, Y. Shao-Horn, *Energy Environ. Sci.* **2013**, *6*, 750.
[7] F. Cheng, J. Chen, *Chem. Soc. Rev.* **2012**, *41*, 2172.
[8] B. Sun, X. Huang, S. Chen, P. Munroe, G. Wang, *Nano Lett.* **2014**, *14*, 3145.
[9] M. Leskes, N. E. Drewett, L. J. Hardwick, P. G. Bruce, G. R. Goward, C. P. Grey, *Angew. Chem., Int. Ed.* **2012**, *51*, 8560.
[10] S. A. Freunberger, Y. Chen, Z. Peng, J. M. Griffin, L. J. Hardwick, F. Bardé, P. Novák, P. G. Bruce, *J. Am. Chem. Soc.* **2011**, *133*, 8040.
[11] D. Xu, Z.-L. Wang, J.-J. Xu, L.-L. Zhang, L.-M. Wang, X.-B. Zhang, *Chem. Commun.* **2012**, *48*, 11674.
[12] W. Walker, V. Giordani, J. Uddin, V. S. Bryantsev, G. V. Chase, D. Addison, *J. Am. Chem. Soc.* **2013**, *135*, 2076.
[13] Z. Peng, S. A. Freunberger, Y. Chen, P. G. Bruce, *Science* **2012**, *337*, 563.
[14] J.-J. Xu, Z.-L. Wang, D. Xu, L.-L. Zhang, X.-B. Zhang, *Nat. Commun.* **2013**, *4*, 2438
[15] Z.-L. Wang, D. Xu, J.-J. Xu, L.-L. Zhang, X.-B. Zhang, *Adv. Funct. Mater.* **2012**, *22*, 3699.
[16] H. Lim, Y. Park, H. Song, E. Y. Jang, H. Gwon, J. Kim, Y. H. Kim, M. D. Lima, R. O. Robles, X. Lepró, R. H. Baughman, K. Kang, *Adv. Mater.* **2013**, *25*, 1348.
[17] Y. Cui, Z. Wen, Y. Liu, *Energy Environ. Sci.* **2011**, *4*, 4727.
[18] T. Zhang, H. Zhou, *Angew. Chem., Int. Ed.* **2012**, *51*, 11062.
[19] J. Xie, X. Yao, I. P. Madden, D. E. Jiang, L. Y. Chou, C. K. Tsung, D. Wang, *J. Am. Chem. Soc.* **2014**, *136*, 8903.
[20] H.-G. Jung, J. Hassoun, J.-B. Park, Y.-K. Sun, B. Scrosati, *Nat. Chem.* **2012**, *4*, 579.
[21] F. Li, D. Tang, Z. Jian, D. Liu, D. Golberg, A. Yamada, H. Zhou, *Adv. Mater.* **2014**, *26*, 4659.
[22] R. R. Mitchell, B. M. Gallant, C. V. Thompson, Y. ShaoHorn, *Energy Environ. Sci.* **2011**, *4*, 2952
[23] M. M. Ottakam Thotiyl, S. A. Freunberger, Z. Peng, P. G. Bruce, *J. Am. Chem. Soc.* **2013**, *135*, 494.
[24] B. D. McCloskey, A. Speidel, R. Scheffler, D. C. Miller, V. Viswanathan, J. S. Hummelshøj, J. K. Nørskov, A. C. Luntz, *J. Phys. Chem. Lett.* **2012**, *3*, 997.
[25] A. Riaz, K.-N. Jung, W. Chang, S.-B. Lee, T.-H. Lim, S.-J. Park, R.-H. Song, S. Yoon, K.-H. Shin, J.-W. Lee, *Chem. Commun.* **2013**, *49*, 5984.
[26] A. Riaz, K. N. Jung, W. Chang, K. H. Shin, J. W. Lee, *ACS Appl. Mater. Interfaces* **2014**, *6*, 17815.
[27] X. Lin, Y. Shang, T. Huang, A. Yu, *Nanoscale* **2014**, *6*, 9043.
[28] Y. J. Jun, S. H. Park, S. I. Woo, *ACS Comb. Sci.* **2014**, *16*, 670.
[29] F. J. Li, D. M. Tang, Z. L. Jian, D. Q. Liu, D. Golberg, A. Yamada, H. S. Zhou, *Adv. Mater.* **2014**, *26*, 4659.
[30] G. Zhao, R. Mo, B. Wang, L. Zhang, K. Sun, *Chem. Mater.* **2014**, *26*, 2551.
[31] F. Li, D. Tang, Y. Chen, D. Golberg, H. Kitaura, T. Zhang, A. Yamada, H. Zhou, *Nano Lett.* **2013**, *13*, 4702.
[32] R. Black, S. H. Oh, J. H. Lee, T. Yim, B. Adams, L. F. Nazar, *J. Am. Chem. Soc.* **2012**, *134*, 2902.
[33] Q.-C. Liu, J.-J. Xu, Z.-W. Chang, X.-B. Zhang, *J. Mater. Chem. A* **2014**, *2*, 6081.
[34] Y. Chen, S. A. Freunberger, Z. Peng, O. Fontaine, P. G. Bruce, *Nat. Chem.* **2013**, *5*, 489.
[35] J. Liu, M. N. Banis, Q. Sun, A. Lushington, R. Li, T. K. Sham, X. Sun, *Adv. Mater.* **2014**, *26*, 6358.
[36] L. Zhao, X. Yu, J. Yu, Y. Zhou, S. N. Ehrlich, Y.-S. Hu, D. Su, H. Li, X.-Q. Yang, L. Chen, *Adv. Funct. Mater.* **2014**, *24*, 5557.
[37] L. Shen, E. Uchaker, X. Zhang, G. Cao, *Adv. Mater.* **2012**, *24*, 6502.
[38] W. Ai, Z. M. Luo, J. Jiang, J. H. Zhu, Z. Z. Du, Z. X. Fan, L. H. Xie, H. Zhang, W. Huang, T. Yu, *Adv. Mater.* **2014**, *26*, 6186.
[39] L. Zhang, H. B. Wu, Y. Yan, X. Wang, X. W. Lou, *Energy Environ. Sci.* **2014**, *7*, 3302.
[40] F. Li, D. Tang, Z. Jian, D. Liu, D. Golberg, A. Yamada, H. Zhou, *Adv. Mater.* **2014**, *26*, 4659.
[41] S. A. Freunberger, Y. Chen, N. E. Drewett, L. J. Hardwick, F. Bard´e, P. G. Bruce, *Angew. Chem., Int. Ed.* **2011**, *50*, 8609.
[42] H.-G. Jung, J. Hassoun, J.-B. Park, Y.-K. Sun, B. Scrosati, *Nat. Chem.* **2012**, *4*, 579.
[43] Y. Chen, S. A. Freunberger, Z. Peng, F. Bardé, P. G. Bruce, *J. Am. Chem. Soc.* **2012**, *134*, 7952.
[44] B. D. Adams, C. Radtke, R. Black, M. L. Trudeau, K. Zaghib, L. F. Nazar, *Energy Environ. Sci.* **2013**, *6*, 1772.
[45] R. Black, J.-H. Lee, B. Adams, C. A. Mims, L. F. Nazar, *Angew. Chem., Int. Ed.* **2013**, *52*, 392.
[46] B. M. Gallant, D. G. Kwabi, R. R. Mitchell, J. Zhou, C. V. Thompson, Y. Shao-Horn, *Energy Environ. Sci.* **2013**, *6*, 2518.
[47] H. Jung, H. Kim, J. Park, I. Oh, J. Hassoun, C. S. Yoon, B. Scrosati, Y. Sun, *Nano Lett.* **2012**, *12*, 4333.
[48] E. Yilmaz, C. Yogi, K. Yamanaka, T. Ohta, H. R. Byon, *Nano Lett.* **2013**, *13*, 4679.
[49] H.-K. Lim, H.-D. Lim, K.-Y. Park, D.-H. Seo, H. Gwon, J. Hong, W. A. Goddard, H. Kim, K. Kang, *J. Am. Chem. Soc.* **2013**, *135*, 9733.
[50] Z.-H. Cui, X.-X. Guo, H. Li, *Energy Environ. Sci.* **2015**, *8*, 182.

© 2016 WILEY-VCH Verlag GmbH & Co. KGaA, Weinheim